Graefe's Archive for Clinical and Experimental Ophthalmology (2021) 259:101–111
https://doi.org/10.1007/s00417-020-04887-2

BASIC SCIENCE

Retinal pigment epithelial responses based on the irradiation density of selective retina therapy

Seung Hee Jeon[1] · Minhee Kim[1] · Young-Jung Roh[1]

Received: 15 May 2020 / Revised: 15 July 2020 / Accepted: 6 August 2020 / Published online: 14 August 2020
© Springer-Verlag GmbH Germany, part of Springer Nature 2020

Abstract

Purpose We evaluated the response of the retinal pigment epithelium (RPE) to high-density (HD) or low-density (LD)-selective retina therapy (SRT) with real-time feedback-controlled dosimetry (RFD) in rabbits.

Methods Sixteen eyes of 8 Chinchilla Bastard rabbits underwent SRT with RFD (527-nm wavelength, 1.7-μs pulse duration), using automatically titrated pulse energy, by using optoacoustic dosimetry or real-time reflectometry. Fifty-six 25-μJ SRT, including LD-SRT (1-spot or 2-spot-spacing) and HD-SRT (4-spot, 7-spot, or 9-spot-no-spacing), were applied per eye. Color fundus photography and fundus fluorescein angiography (FFA) were used to confirm SRT spots 1-h post-SRT. Light microscopy and scanning electron microscopy (SEM) were performed at 2-h, 3-day, 7-day, and 1-month post-treatment.

Results We tested 896 spots irradiated by SRT with RFD and confirmed that SRT lesions were adequate, based on invisibility on fundoscopy and visibility on FFA. On SEM, at 2-h post-SRT, flattened RPE cells were observed in the center of the SRT lesion. While normal RPE cells were clearly observed between LD-SRT lesions, healthy RPE cells were rare in HD-SRT lesions at 2-h post-treatment. At 7-day post-SRT, SEM revealed completely restored LD-SRT lesions with small or large RPE cells with microvilli, whereas HD-SRT lesions were covered with RPE cells without microvilli. At 1-month post-SRT, SEM revealed restored RPE cells with microvilli in HD-SRT lesions. On light microscopy, both HD- and LD-SRT lesions were completely restored with adjacent RPE cells and spared photoreceptors at 1-month post-treatment.

Conclusions Although both HD- and LD-SRT lesions had recovered at 1-month post-SRT, LD-SRT lesions healed faster than HD-SRT lesions.

Keywords Microvilli · Photoreceptors · Real-time feedback-controlled dosimetry (RFD) · Retinal pigment epithelium (RPE) · Selective retina therapy (SRT)

Introduction

Conventional laser photocoagulation has shown favorable clinical results in the treatment of diabetic retinopathy [1, 2]. Since it is associated with serious complications, such as central scotoma due to photoreceptor damage, progressive enlargement of the laser scar, and choroidal neovascularization, the use of conventional laser photocoagulation has been limited to treating patients with macular diseases [3, 4]. To avoid side effects, selective retina therapy (SRT) has been developed to allow selective damage to the retinal pigment epithelium (RPE), while sparing the adjacent neurosensory retina [5, 6]. Although the precise mechanism of SRT is not known, the beneficial effect of SRT is thought to be associated with the creation of a new RPE barrier, the so-called outer blood–retinal barrier, at SRT-treated areas and the release of cell mediators such as matrix metalloproteinase-2 and pigment epithelium-derived factor during RPE regeneration [7, 8].

Selective RPE damage is achieved when SRT with a 1.7-μs pulse duration is absorbed mainly by melanosomes in RPE cells. Since the effect of SRT is confined to RPE cells, without affecting the surrounding retinal tissue, well-titrated SRT does not induce instantly visible changes on ophthalmoscopy [9]. If the pulse energy of SRT is irradiated without appropriate titration, SRT can produce visible burns on the retina. Therefore, two therapeutic endpoints, viz., adequate SRT

✉ Young-Jung Roh
youngjungroh@hanmail.net

[1] Department of Ophthalmology and Visual Science, Yeouido St. Mary's Hospital, College of Medicine, The Catholic University of Korea, 10, 63-ro, Yeongdeungpo-gu, Seoul 07345, Republic of Korea

Key messages

Selective retina therapy (SRT) induces RPE rejuvenation by restoring a new RPE layer at SRT-treated area. Our rabbit experiment demonstrated that that both high- and low-density SRT lesions were fully covered with RPE with microvilli at 1-month post-SRT. Although high-density SRT lesions showed slower healing than low-density lesions, high-density irradiation of SRT enlarged the area of new RPE layer, while sparing photoreceptors and Bruch's membrane.

spots that are invisible on ophthalmoscopy but visible on fundus fluorescein angiography (FFA), have been used for SRT application [5, 6, 9]. SRT was irradiated after titrating adequate pulse energy, based on the angiographic and ophthalmoscopic features of test spots nearby temporal arcade vessels, in previous studies [10–12]. Although overtreatment did not occur when the pulse energy was determined based on these two endpoints, undertreatment was occasionally observed at the SRT-treated area, due to the anatomical difference between the healthy tested area and the thickened macula, with macular edema or subretinal fluid [11, 12].

To find the adequate pulse energy of SRT without performing pretreatment FFA, real-time feedback-controlled dosimetry (RFD), operated by both optoacoustic dosimetry and reflectometry, has been developed to detect microbubbles originating from RPE damage in real-time during irradiation. Briefly, optoacoustic dosimetry provides the optoacoustic feedback value (OAV) by detecting the ultrasonic pressure from microbubbles during irradiation [5, 13]. Reflectometry provides the optical feedback reflectometric value (RMV) by detecting the reflection of backscattered light from microbubbles [6, 11, 14, 15]. The OAV and RMV originating from microbubbles within RPE cells can be monitored by RFD that implements optoacoustic and reflectometric sensors. Although various pulse energies have been used in a previous rabbit experiment, RFD was useful to produce the adequate SRT lesions [6, 14].

In previous studies, SRT spots of 160- or 200-μm diameter were completely restored by the adjacent, untreated RPE cells within 1 week, based on histology [5, 6, 14]. Since the mechanism of SRT is known to be associated with new RPE restoration, by building a new outer blood-retinal barrier, high-density SRT (HD-SRT) with no-spacing irradiation might be more useful for inducing a wider new RPE monolayer area than low-density SRT (LD-SRT). However, the adjacent, untreated RPE cells between SRT lesions are thought to play a crucial role in RPE restoration, as a first reaction to SRT [7, 8, 14]; therefore, RPE restoration could be affected if the number of neighboring healthy RPE cells is decreased by HD-SRT. Our goal was to compare the RPE responses to HD-SRT or LD-SRT in a rabbit experiment, as these responses have not been compared with date.

Methods

Animals

Sixteen eyes of 8 Chinchilla Bastard rabbits (4–6 months old, 1.8–2.3 kg) received SRT with RFD. The rabbits were anesthetized with combinations of zoletil® (Vibrac, Carros, France; 0.2 mg/kg body weight) and xylazine hydrochloride (5 mg/kg). Topical 0.5% tropicamide (Tropamide, Bilim, Turkey) was used to dilate the pupils. The animals in this experiment were treated in accordance with the ARVO Statement for the Use of Animals in Ophthalmic and Vision Research, and this study was approved by the Institutional Animal Care and Use Committee of the Catholic University of Korea.

Selective retina therapy

Sixteen eyes underwent both HD-SRT and LD-SRT (Q-switched Nd:YLF 527-nm laser, 1.7-μs micropulse duration, 100-Hz frequency, 200-μm diameter), delivered via an SRT laser system with RFD (R:GEN, Lutronic, Goyang-si, South Korea). The laser emits 15 micropulses per spot, with ramping: in each burst, the first micropulse energy is 50% of that of the 15th micropulse energy, and the pulse energy of the subsequent micropulses is increased by an additional 3.57%. The 15th micropulse energy can be controlled by the clinician as a preset pulse energy, as previously described [14].

As the preset pulse energy is raised, the high-peak temperature at the melanosome generates microbubbles that disrupt RPE cells mechanically. The signals from the microbubbles can be detected by RFD with optoacoustic and reflectometric sensors, which provide the OAV and RMV in real time, in arbitrary units (AUs). The OAV and RMV are considered to be "above threshold" as soon as they exceeds each

predetermined value of RFD-va1.1 (OAV: 1.0 AU, RMV: 1.2 AU) [14]. As soon as the OAV or RMV reaches the threshold, the subsequent micropulses cease automatically, according to the signal processing algorithm of RFD-va1.1. The energy of autostopped micropulses indicating detection of microbubbles is referred to as the selective micropulse energy. The placement of selective micropulses among the 15 micropulses was recorded during each irradiation in this study. The pulse energy of SRT was preset to 25 μJ, and the real-applied energy was calculated according to the varied placement of selective micropulse energies.

The "adequate" SRT spots were confirmed by color fundus photography (CFP) and FFA [5, 6]. The various treatment patterns, including LD-SRT (1-spot or 2-spot-spacing irradiation) and HD-SRT (4-spot-, 7-spot-, or 9 spot-no-spacing irradiation), were delivered to each eye by using SRT implemented software (Table 1). To provide the orientation for the invisible SRT irradiation and tissue pathology, three marker burns of 140 μJ were initially applied after turning off the RFD, after which additional 11 marker burns were irradiated in the inferior parapapillary retina. After turning on the RFD, 56 SRT spots (25 μJ) were applied between marker burns in each eye (Fig. 1a).

Diagnostic and histological evaluation

In all rabbits, CFP and FFA (TRC-50DX, Topcon Corp., Tokyo, Japan) were used to confirm the SRT spots 1 h after SRT. FFA was performed with intravenous injection of 0.5 mL of 10% fluorescein (Fluorescite; Alcon Laboratories, Hünenberg, Switzerland) via the ear vein. Any instantly visible changes at the SRT lesions were interpreted as a burn. The rabbits were sacrificed with an overdose of KCL at different time-points after SRT, and then eyes were enucleated for histologic evaluation (Table 1). By using landmarks, such as the optic nerve head and marker burns, tissue pathology could include both marker burns and SRT lesions. Following the removal of the anterior parts of the eyes, the lens, and the vitreous, the tissue of the posterior eyecup was prepared by immersion fixation in 4% glutaraldehyde for 2 days. The tissue was dehydrated in ethanol and embedded. Hematoxylin and eosin staining of 5-μm sections was performed for light microscopy, as previously described [6].

For scanning electron microscopy (SEM), the posterior eyecup was cut from the anterior part of the globe and the posterior cup was immersed in saline solution for 40 min. After carefully peeling the retina from the RPE layer, the remaining eyecup, including the sclera, choroid, and RPE, was fixed in 2.5% glutaraldehyde in phosphate-buffered saline (PBS) for 2 h at 4 °C. After several rinses in PBS, a 2-h postfix with 2% osmium tetroxide was performed at 4 °C. Samples were washed in distilled water and dehydrated in an ethanol series, and then the specimens were freeze-dried ES-2030, Hitachi, Tokyo, Japan) and coated with platinum in an ion coater (Eiko IB-5, Tokyo, Japan) for SEM observation (S-4700, Hitachi). SEM was used to observe SRT lesions in the assigned eyes at 2 h, 3 days, 7 days, and 1 month after treatment.

The rate of detection of RPE damage, as a measure of the sensitivity of RFD, was calculated from the ratio of the

Table 1 Summary of rabbit eyes used in this study

Rabbit no.	OD/OS	Total no. of SRT spots	Time of histologic exam after SRT treatment	Present pulse energy of SRT spots (μJ)	Mean real-applied pulse energy of SRT spots (μJ ± S.D.)
1	OD	56	2 h (LM)	25	18.7 ± 3.2
	OS	56	2 h (SEM)	25	18.4 ± 2.0
2	OD	56	2 h (SEM)	25	18.4 ± 2.2
	OS	56	2 h (SEM)	25	19.0 ± 1.9
3	OD	56	3 days (SEM)	25	18.8 ± 1.3
	OS	56	3 days (LM)	25	18.3 ± 1.9
4	OD	56	3 days (SEM)	25	18.4 ± 1.8
	OS	56	3 days (SEM)	25	18.6 ± 1.7
5	OD	56	7 days (LM)	25	18.3 ± 1.5
	OS	56	7 days (SEM)	25	17.8 ± 2.1
6	OD	56	7 days (SEM)	25	18.9 ± 2.1
	OS	56	7 days (SEM)	25	18.6 ± 1.3
7	OD	56	1 month (LM)	25	20.1 ± 2.4
	OS	56	1 month (SEM)	25	19.7 ± 2.2
8	OD	56	1 month (SEM)	25	18.0 ± 1.9
	OS	56	1 month (SEM)	25	17.7 ± 1.6

SRT selective retina therapy, *LM* light microscopy, *SEM* scanning electron microscopy

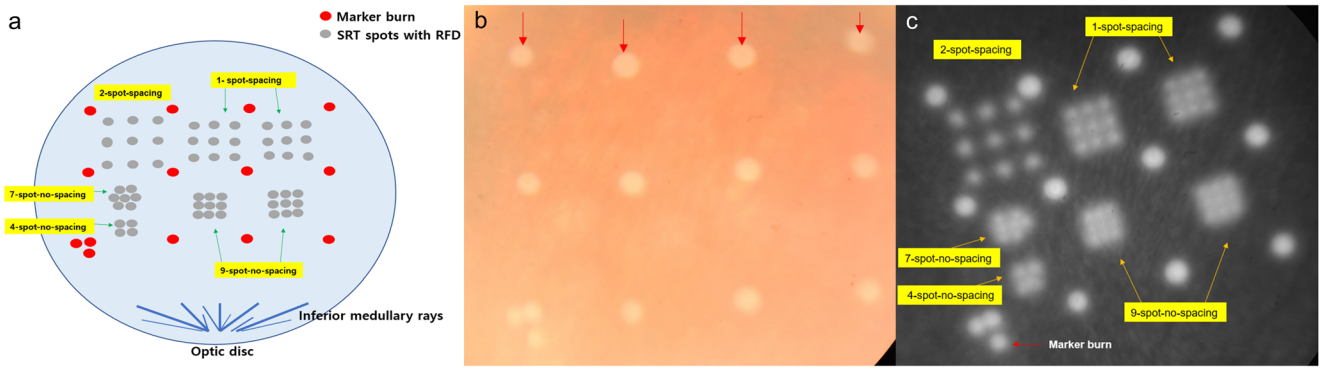

Fig. 1 Representative treatment protocol of selective retina therapy (SRT) with real-time feedback-controlled dosimetry (RFD). **a** The treatment map for SRT spots (gray color) with low-density irradiation (1-spot-, 2-spot-spacing) and high-density irradiation (4-spot-, 7-spot-, 9-spot-no-spacing) and 14 marker burns (red color). **b** Marker burns (red arrow) of 140 μJ show a whitish discoloration, whereas 56 SRT lesions are invisible on color fundus photography at 1 h after SRT. Three marker burns are used as a landmark. **c** Both marker burns (red arrow) and SRT spots (yellow arrows) show hyperfluorescence on fundus fluorescein angiography at 1 h after SRT

number of adequate FFA-visible SRT spots above the threshold to the number of all FFA-visible spots, as previously described [12, 14]. The specificity of RFD was defined as the ratio of the number of FFA-invisible SRT spots below the threshold to the number of all FFA-invisible spots.

Results

Fundus examination and fluorescein angiography

While all 224 marker burns (140 μJ) produced a whitish discoloration during irradiation, none of the 896 SRT spots (25 μJ) showed any visible change on ophthalmoscopy. On CFP, at 1 h after laser treatment, all marker burns showed whitish lesions in all rabbits, whereas all SRT spots were invisible (Fig. 1b). On FFA, at 1 h after SRT, SRT spots showed hyperfluorescence (Fig. 1c). All SRT spots were regarded as "adequate" based on the two endpoints defined in this study.

Scanning electron microscopy and light microscopy

On SEM, at 2 h after SRT, flattened RPE cells without microvilli were observed in the center of SRT lesions, whereas RPE cells with abundant microvilli were observed in untreated areas (Fig. 2a). While marker burns showed large destroyed lesions with irregular margins, SRT lesions revealed relatively small and well-delineated lesions on SEM. The LD-SRT and HD-SRT lesions were clearly shown because of the abrupt margin of the RPE-damaged area. HD-SRT produced wider lesions than LD-SRT lesions on SEM at 2 h. Among HD-SRT lesions, 9-spot-no-spacing lesions were larger than the 4- or 7-spot-no-spacing lesions (Fig. 2a, b). No disruption of Bruch's membrane was observed at either LD-SRT or HD-SRT lesions (Fig. 2a, c).

Low-density SRT lesions

On SEM, 3 days after SRT, the lesions were partly covered with polygonal RPE cells (Fig. 2d). Flattened RPE cells without microvilli were observed in the center of SRT lesions at 3 days post-treatment (Fig. 2e). At 7 days after SRT, 2-spot-spacing LD-SRT lesions were fully restored, and small and large RPE cells with microvilli and multilayered RPE cells were observed on SEM (Fig. 2f, g). On light microscopy, 2 h after treatment, SRT lesions showed slightly relaxed photoreceptor outer segments while sparing the inner retinal layer and Bruch's membrane (Fig. 2h).

Overall, the healing process of 1-spot-spacing SRT lesions was similar to that of 2-spot-spacing lesions. The untreated areas between 1-spot-spacing SRT lesions were smaller than that between 2-spot-spacing SRT lesions because of the increased density of the SRT spots (Fig. 3a). LD-SRT lesions with 1-spot spacing were partly covered with small or large elongated RPE cells at 3 days after SRT (Fig. 3b, c). On SEM, at 7 days after SRT, the LD-SRT lesions were fully restored, with an increased number of small RPE cells with microvilli (Fig. 3d, e). On light microscopy, at 3 days after SRT, while marker burns revealed full thickness destruction of retinal tissue, LD-SRT lesions with 1-spot spacing showed selective RPE damage and relaxed photoreceptor outer segments, while the inner retinal layer was spared (Fig. 3f).

High-density SRT lesions

On SEM, at 2 h after SRT, 7-spot-no-spacing HD-SRT lesions were larger than 4-spot-no-spacing lesions (Fig. 4a). In the center of the HD-SRT lesion, the normal RPE cells between SRT lesions were scarce, although Bruch's membrane was intact (Fig. 4b). At 3 days after SRT, flattened RPE cells without microvilli were observed in the center of 4- and 7-spot-no-spacing lesions on SEM (Fig. 4c, d). At 7 days after

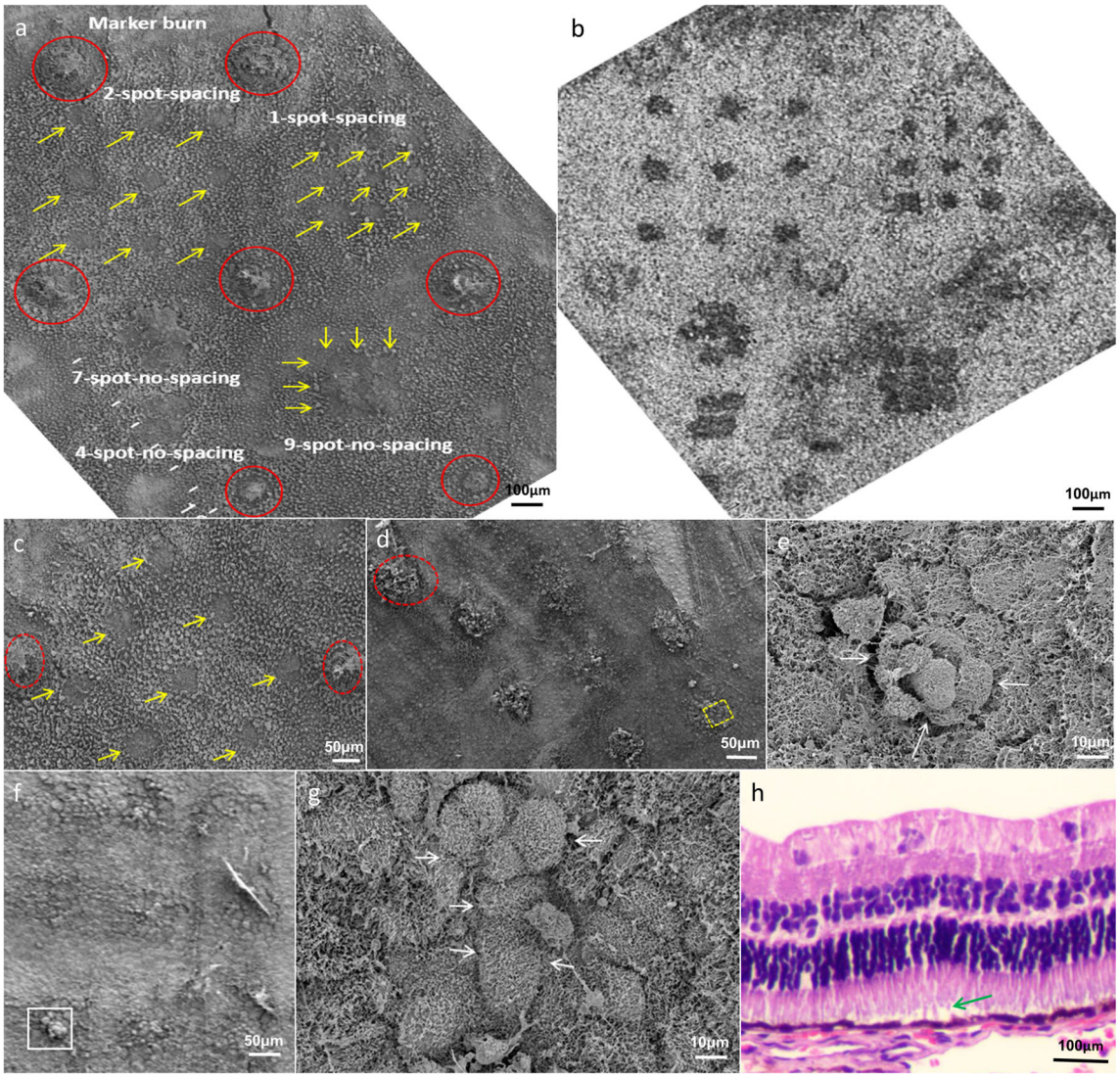

Fig. 2 The tissue reaction to low-density (LD) and high-density (HD) selective retina therapy (SRT) irradiation. **a** On scanning electron microscopy (SEM) at 2 h after SRT, SRT lesions (yellow arrows) are visible between marker burns (red circles). Flattened retinal pigment epithelium (RPE) cells without microvilli are observed in the center of SRT lesions, and normal RPE cells with microvilli are observed in untreated areas at 2 h after SRT. **b** HD-SRT with no-spacing irradiation produces larger RPE-damaged areas than LD-SRT with spacing irradiation, in the inverted image of figure (**a**). **c** Unlike the destroyed retinal tissue at the marker burns (red circles) seen on SEM at 2 h after SRT, 2-spot-spacing SRT lesions (yellow arrows) show a relatively well-delineated RPE-damaged area. Bruch's membrane is intact in the center of the SRT lesions. **d** On SEM, at 3 days after SRT, SRT lesions (yellow square) are partly covered with polygonal RPE cells. **e** In the magnified image, elongated and multi-layered RPE cells (white arrows) without microvilli are observed in the center of the SRT lesion at 3 days after treatment. **f** The LD-SRT lesions are fully restored, with polygonal small RPE cells (white square) on SEM at 7 days after SRT. **g** In the magnified image, multilayered RPE cells (white arrows) with microvilli are observed in the center of the LD-SRT lesion. **h** On light microscopy, at 2 h after SRT, 2-spot-spacing LD-SRT lesion (green arrow) shows a slightly relaxed photoreceptor outer segment, with sparing of the inner retinal layer and Bruch's membrane

SRT, HD-SRT lesions were fully restored by small or large RPE cells without microvilli, as seen on SEM (Fig. 4e, f). On light microscopy, at 7 days after HD-SRT, focal multilayered RPE cells were observed in the 7-spot-no-spacing lesions and the photoreceptor layer was intact (Fig. 4g). The healing process of HD-SRT lesions with 9-spot-no-spacing was similar to that of other no-spacing HD-SRT lesions (Fig. 5). While HD-SRT lesions were restored with polygonal RPE cells without microvilli at 7 days, HD-SRT lesions were completely restored with small RPE cells with microvilli, as seen on SEM, at 1 month after SRT (Fig. 5f, g). On light microscopy, at 1 month after HD-SRT, 9-spot-no-spacing lesions showed a normal retinal structure with focal, multilayered RPE cells (Fig. 5h).

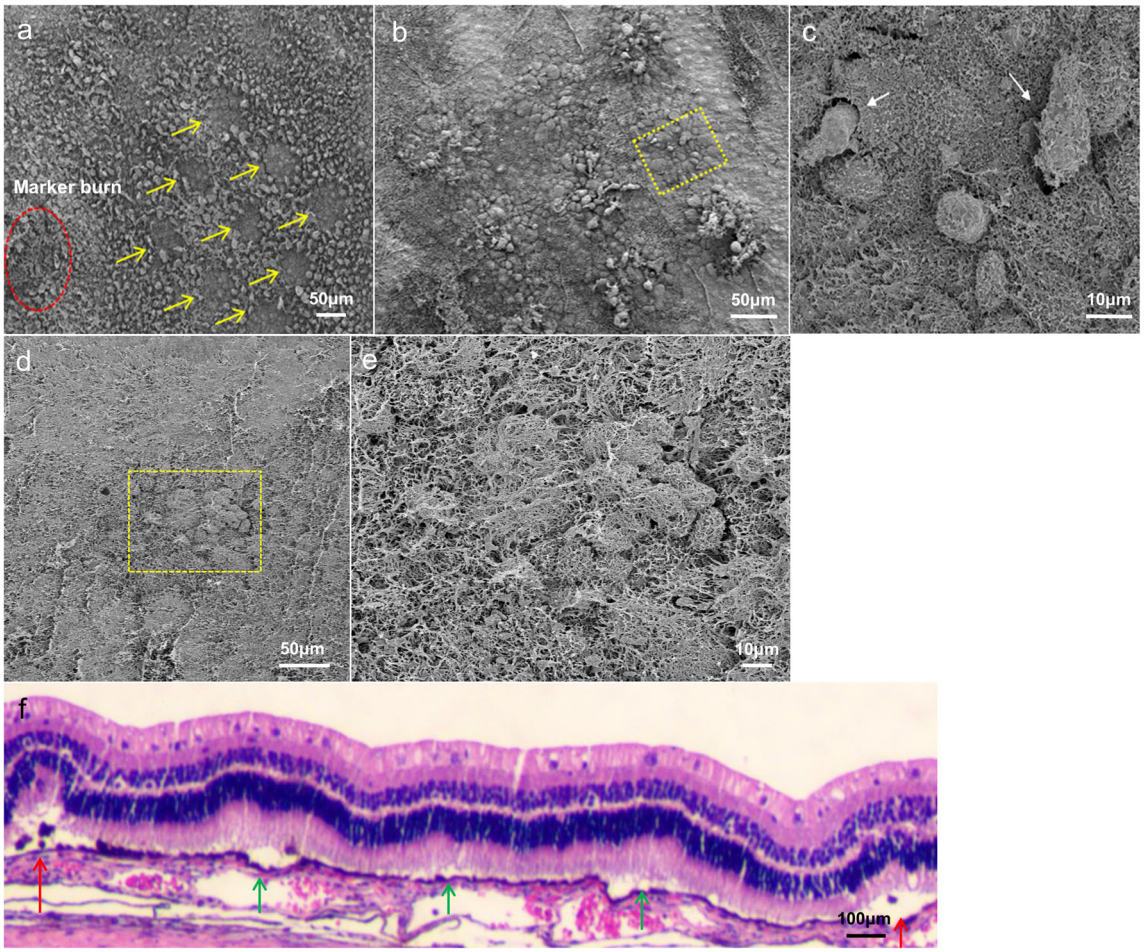

Fig. 3 The tissue reaction to low-density selective retina therapy (LD-SRT) with 1-spot-spacing irradiation and marker burns. **a** On scanning electron microscopy (SEM), at 2 h after SRT, the normal retinal pigment epithelium (RPE) cells between 1-spot-spacing SRT lesions (yellow arrows) are smaller than that between 2-spot-spacing lesions, due to the increased density of SRT spots. No disruption of Bruch's membrane is observed at SRT lesions. **b** On SEM, at 3 days after treatment, SRT lesions are not completely covered with polygonal RPE cells. **c** In the magnification of image **b** (yellow square), the elongated RPE cells without microvilli (white arrows) are observed at the margin of SRT lesion 3 days after SRT. **d** On SEM 7 days after SRT, the SRT lesions are fully covered with monolayered or multilayered small RPE cells. **e** An increased number of polygonal small RPE cells with microvilli are observed at the SRT lesion in the magnified of image (**d**) (yellow square). **f** On light microscopy, at 3 days after SRT, marker burns (red arrows) show a full-thickness destruction of retinal tissue, whereas SRT lesions (green arrows) show a selective disruption of photoreceptor outer segments, while the inner retinal layer is spared

Real-time feedback-controlled dosimetry

The OAV and RMV of 896 SRT spots were analyzed with CFP and FFA. None of the SRT spots showed any "visible" changes on CFP in this study. The rate of detection of RPE damage, representing the sensitivity of RFD, was 96.1% (861/896 spots), because 35 FFA-positive spots below the threshold did not induce the auto-stop. These 35 SRT spots were also invisible on ophthalmoscopy and could be detected only by weak hyperfluorescence on FFA at 1 h after SRT. The specificity could not be calculated because all SRT spots were FFA-visible spots. In addition, since the placement of 861 auto-stopped SRT spots occurred between the 1st and 15th micropulse during irradiation, the mean real-applied pulse energy of SRT was lower than that of the mean preset pulse energy (25 μJ) in all rabbits (Fig. 6b).

Discussion

Although the effect of SRT is associated with various cell mediators during the process of healing of an RPE-damaged area, the complete restoration of a new outer blood-retinal barrier is known to be crucial to the mechanism underlying the effects of SRT [5, 7, 8]. No previous study has investigated the RPE responses to LD-SRT and HD-SRT irradiation in a rabbit experiment. Our results demonstrated that both HD-SRT and LD-SRT lesions were completely covered by new polygonal RPE cells by 1 month after SRT. However, HD-SRT lesions may heal slower than LD-SRT lesions.

The effects of RPE cell debridement on the photoreceptor–RPE–choriocapillaris interface have been investigated in animal experiments [16–19]. The area of RPE debridement via subretinal surgery or laser photocoagulation was repopulated

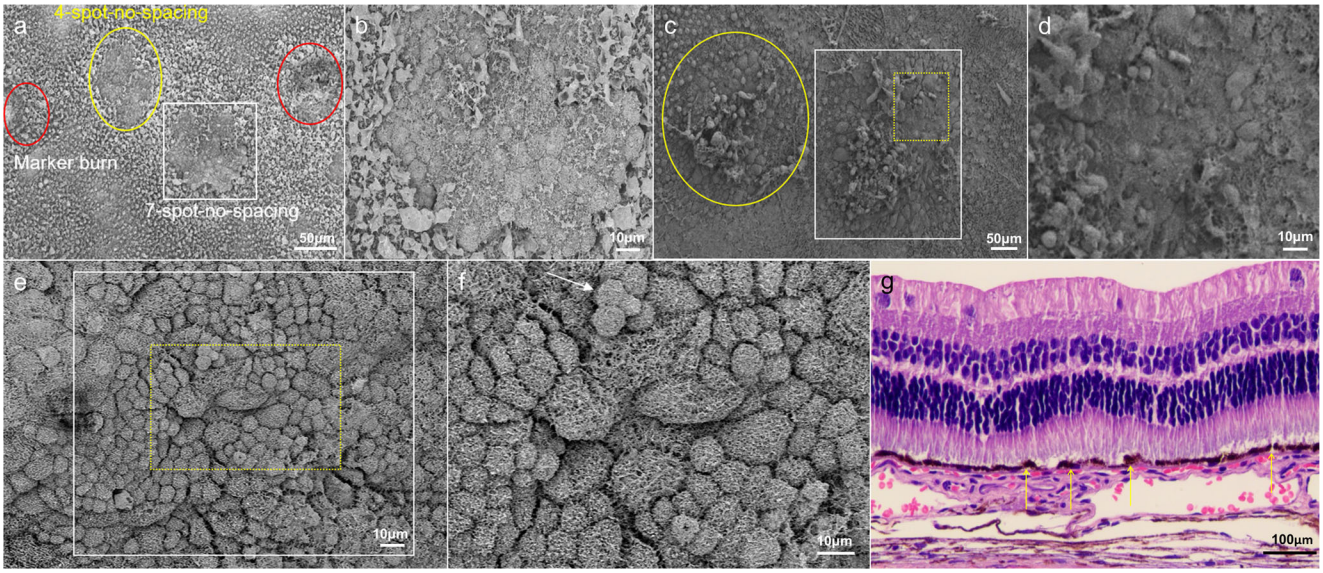

Fig. 4 The tissue reaction to high-density selective retina therapy (HD-SRT) with 4- and 7-spot-no-spacing irradiation. **a** On scanning electron microscopy (SEM), at 2 h after SRT, a 7-spot-no-spacing SRT lesion (white square) is larger than a 4-spot-no-spacing lesion (yellow circle). No disruption of Bruch's membrane is observed at HD-SRT lesions. Marker burns (red circles) show a denuded RPE layer and destroyed retinal tissue. **b** In the magnified image of the 7-spot-no-spacing HD-SRT lesion (white square), flattened RPE cells and cellular debris are observed in the center of the SRT lesion. Normal appearing RPE cells within HD-SRT lesions are scarce. **c** On SEM, at 3 days after SRT, the flattened RPE cells without microvilli are observed in 4-spot-no-spacing (yellow circle) and 7-spot-no-spacing (white square) lesions. **d** In the magnification of image (**c**) (yellow square), in the 7-spot-no-spacing lesion, the RPE-damaged area is not covered and flattened RPE cells without microvilli are seen at 3 day post-treatment. **e** On SEM, at 7 days after SRT, the 7-spot-no-spacing lesion (white square) is fully restored with polygonal RPE cells. **f** In the magnification of image (**e**) (yellow square), polygonal RPE cells without microvilli are observed at 7 days after SRT. Multilayered RPE cells (white arrow) are observed at 7 days post-treatment. **g** On light microscopy, at 7 days after SRT, focal multilayered RPE cells (yellow arrows) are seen in the 7-spot-no-spacing HD-SRT lesion. The photoreceptor inner segments are intact

due to proliferation and migration of peripheral RPE cells in in vivo studies [19–22]. Additionally RPE restoration after denuding RPE cells by using surgical methods was observed if Bruch's membrane was intact, whereas the normal wound healing of RPE cells was interrupted where Bruch's membrane was disrupted, in previous studies [16–18]. Although histological restoration of the RPE layer correlated with recovery of retinal function, based on an electroretinogram test [20], surgical trauma to Bruch's membrane and the choriocapillaris at the retinotomy site caused post-treatment choriocapillary perfusion defects and inadvertent RPE loss [18, 19]. Confined damage to the photoreceptor outer segment was necessary for successful RPE restoration in an experimental model of RPE loss by surgical debridement [16–19], but such precise surgical skill might be somewhat challenging.

Contrary to the RPE restoration after surgical RPE debridement, SRT demonstrated RPE restoration without affecting the neurosensory retina in previous animal experiments [5–9, 14]. Additionally, RPE cell mitosis and proliferation, indicating RPE rejuvenation after SRT, were exhibited previously by using porcine RPE-choroid explants [7, 8]. In the present study, in the center of LD-SRT and HD-SRT lesions, no disruption of Bruch's membrane was observed on SEM at 2 h after SRT. Similarly, on light microscopy at 2 h after SRT, both LD- and HD-SRT lesions showed partial damage to the photoreceptor outer segment while sparing Bruch's membrane. As an undamaged Bruch's membrane is critical for normal RPE repopulation after surgical RPE debridement [16–18], SRT might be useful for inducing RPE restoration, because no disruption of Bruch's membrane was observed after SRT [5, 7, 14]. Although transmission electron microscopy was not employed in this study, light microscopy consistently showed that SRT lesions were confined to the RPE and photoreceptor outer segment at 2-h, 3-day, 7-day, and 1 month post-treatment (Figs. 2h; 3f; 4g; 5h).

RPE restoration after SRT in humans was demonstrated by means of diagnostic modalities, such as FFA, optical coherence tomography, autofluorescence, and microperimetry [11, 12, 23–25]. Briefly, SRT lesions that are FFA-visible immediately following SRT became FFA-invisible at 3-month post-treatment, due to RPE restoration [11]. On fundus autofluorescence, SRT did not induce hypoautofluorescence, indicating RPE atrophy [11, 12, 23]. Additionally, retinal sensitivity after SRT showed no scotomatous changes in prior studies [11, 24, 25]. Although RPE restoration after a single SRT irradiation with a diameter of 160 or 200 μm was clearly demonstrated in animal studies [5, 6, 14], RPE restoration at wider SRT lesions has not been investigated. Given that the SRT lesion was covered by migration and proliferation of normal RPE cells at the margin of the RPE-damaged area [5,

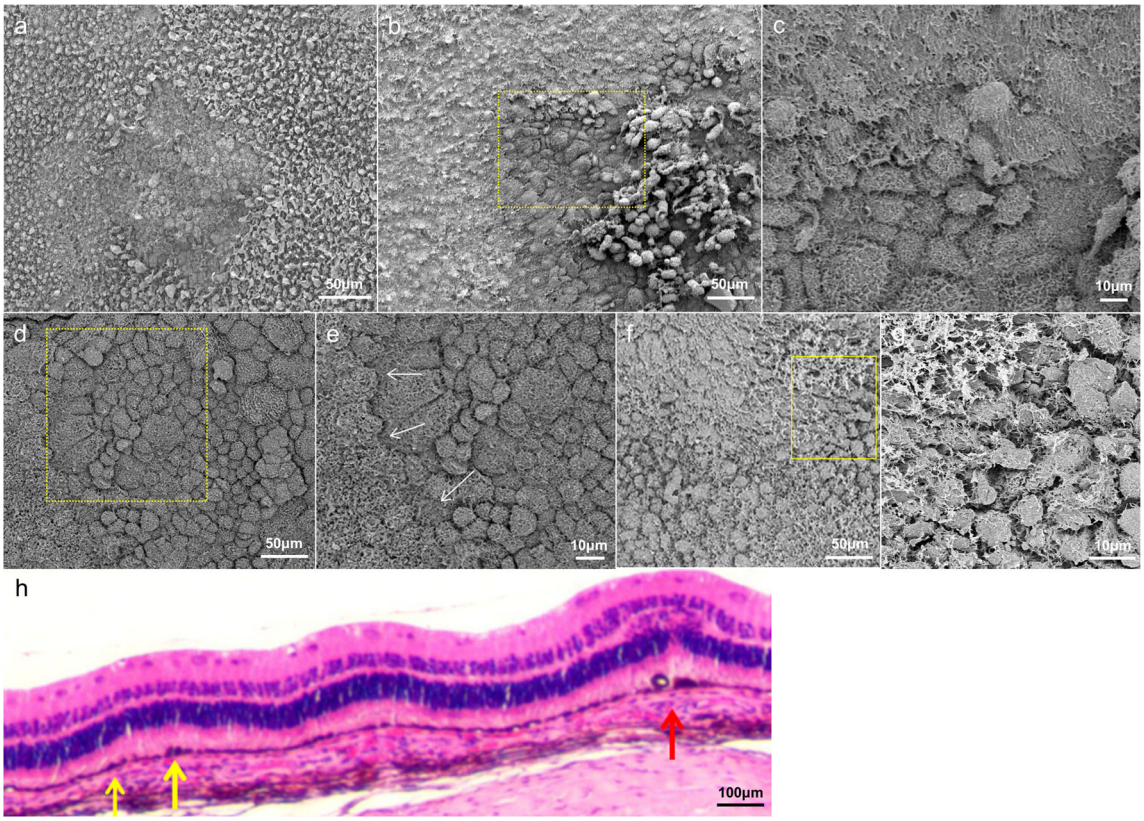

Fig. 5 The tissue reaction to high-density selective retina therapy (HD-SRT) with 9-spot-no-spacing irradiation. **a** On scanning electron microscopy (SEM), at 2 h after SRT, flattened RPE cells are observed in the center of the 9-spot-no-spacing SRT lesion. No disruption of Bruch's membrane is seen at the HD-SRT lesion. **b** The HD-SRT lesion is not covered at 3-day post-treatment. Much cellular debris is observed in the center of the HD-SRT lesion. **c** In the magnification of image (**b**) (yellow square), flattened RPE cells without microvilli are observed in the HD-SRT lesion. **d** On SEM, at 7 days after SRT, the SRT lesion is fully restored with polygonal RPE cells without microvilli. **e** An evident margin (white arrow) between normal RPE cells with microvilli and new polygonal RPE cells without microvilli is seen at 7 days in the magnification of image (**d**) (yellow square). **f** On SEM, at 1 month after SRT, HD-SRT lesions are completed healed, showing polygonal RPE cells. **g** In the magnification of image (**f**) (yellow square), small RPE cells with microvilli are observed at an HD-SRT lesion at 1 month after SRT. **h** On light microscopy, at 1 month after SRT, a marker burn (red arrow) shows full-thickness destruction of retinal tissue, whereas an HD-SRT lesion presents a normal retinal structure with focal multi-layered RPE cells (yellow arrows)

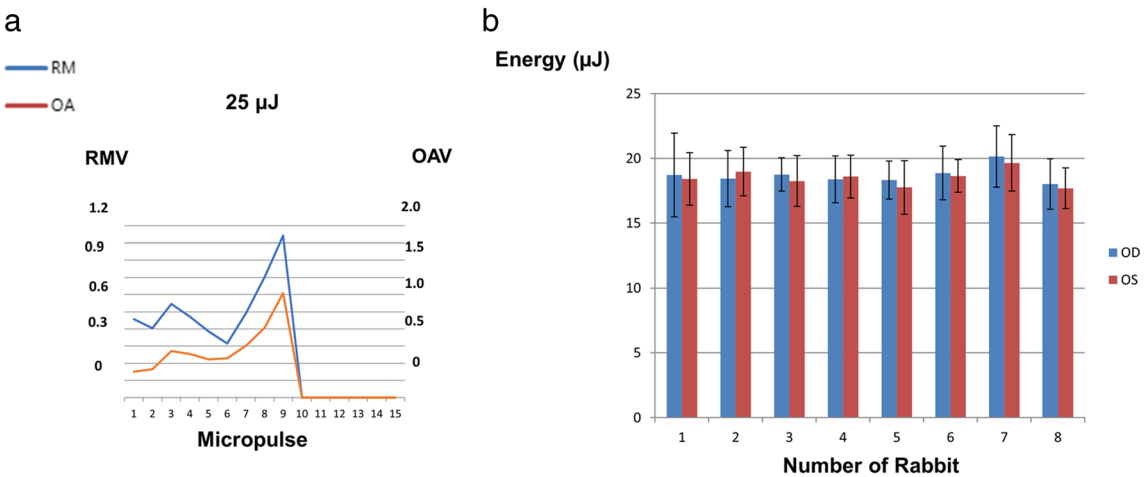

Fig. 6 A representative picture of auto-stop by real-time feed-back dosimetry (RFD). Selective retina therapy (SRT) irradiation ceases automatically when the optoacoustic value (OAV) or reflectometric value (RMV) reaches the threshold level (OAV: 1.0 AU, RMV: 1.2 AU). **a** SRT irradiation (25 μJ) ceases at the 9th of 15 micropulses when the OAV reaches the threshold earlier than the RMV. **b** The mean real-applied energy of 16 rabbit eyes is lower than the present pulse energy (25 μJ), due to the auto-stop of RFD

8, 14], RPE restoration might be affected if the area of normal RPE cells between SRT lesions is reduced by HD-SRT. In the present study, SEM revealed that at 2 h after SRT, HD-SRT lesions showed a larger RPE-damaged area than that of LD-SRT lesions. Although normal RPE cells between HD-SRT lesions were scarce, due to confluent SRT irradiation, as compared with those of LD-SRT lesions (Fig. 2a), both HD-SRT and LD-SRT lesions were fully covered by migration and proliferation of marginal RPE cells at 7 days after treatment, according to SEM observations. LD-SRT lesions were healed, with mostly small RPE cells with microvilli, whereas HD-SRT lesions were covered with polygonal RPE cells without microvilli on SEM images at 7 days after SRT. This finding indicates that the RPE restoration with RPE cells with microvilli in LD-SRT lesions occurs faster than those in HD-SRT lesions. Since the RPE apical microvilli involve RPE functions, including phagocytosis of shed photoreceptor outer segments, transport of nutrients, and visual pigment transport, by interacting with the tips of the rod and cone photoreceptor outer segments [26, 27], restoration of RPE microvilli after SRT is essential for the complete healing of RPE cells. HD-SRT lesions were fully covered with new polygonal RPE cells with microvilli on SEM images at 1 month after SRT in this study. Therefore, SRT could be useful for formulating a new, wider outer blood-retinal barrier, i.e., so-called RPE rejuvenation, by using HD-SRT irradiation.

Short-pulse duration lasers, such as subthreshold nanosecond laser and SRT have been applied to treat dry age-related macular degeneration (AMD) [28–30], based on a similar concept that the RPE layer newly formed after selective RPE damage might be effective for treating AMD. Recently, a multicenter clinical trial showed that subthreshold nanosecond laser played a role in slowing intermediate AMD progression in patients without coexistent reticular pseudodrusen [29]. While both subthreshold nanosecond laser and SRT induce RPE rejuvenation after damaging RPE cells, the outcomes obtained with subthreshold nanosecond laser cannot be applied to SRT, because the former uses different laser parameters and target area. According to the treatment protocol, 12 subthreshold nanosecond laser spots are irradiated just inside the superior and inferior arcade vessels [29], whereas SRT spots are applied at the macular area. In addition to RPE rejuvenation at the SRT-treated area, the effect of SRT might be related to a reduction in Bruch's membrane thickness and AMD-like RPE alterations in AMD mouse models [31]. Therefore, SRT could be a potential therapeutic option for dry AMD, by improving the flux across Bruch's membrane [7, 8, 31].

Subretinal approaches for RPE transplantation in human were associated with a high rate of complications, including retinal detachment, massive membrane formation, and macular hole due to damage to neighboring tissue [32, 33], whereas SRT did not affect retinal function, due to the selectivity of RPE damage, in several clinical studies [11, 12, 24, 25]. The present study also demonstrated that HD-SRT induces RPE restoration while sparing adjacent retinal tissues, including photoreceptors and Bruch's membrane. Since HD-SRT induces a wider area of RPE restoration, with normal appearing RPE cells with microvilli, HD-SRT seems to be more useful for producing wider RPE rejuvenation than LD-SRT. However, considering that the recovery of RPE cells with microvilli was observed at 1-month posttreatment in HD-SRT lesions, as compared with 1-weak post-treatment in LD-SRT lesions, we suspect that the healing process of SRT lesions could be delayed, depending on the density of irradiation.

The effect of SRT on macular diseases, including diabetic macular edema (DME), central serous chorioretinopathy, and geographic atrophy, has been reported in previous clinical studies [10–12, 23–25, 28, 34]. Although SRT resulted in visual improvements in patients with DME, changes in central macular thickness were not significant [10, 11]; furthermore, SRT was more effective against mild DME than severe DME [35]. Since DME was found to be associated with a breakdown of both the inner and outer blood-retinal barriers [36], the restoration of only the outer blood-retinal barrier after SRT might be the reason for its limited efficacy against DME. Additionally, SRT-based irradiation of the surrounding area could not reduce the size of the RPE defect in patients with geographic atrophy, the advanced stage of age-related macular degeneration [37], indicating that the potency of post-SRT RPE proliferation at the margins is not sufficient to heal large geographic atrophy related RPE-defects.

Besides the influence of disease severity on RPE restoration, there are several limitations to applying these animal experiment findings in humans. First, the effect of age was not considered, because young rabbits were used in this study. Since fetal RPE proliferation is much greater than that in older individuals [38], RPE in aged patients with geographic atrophy might be less responsive to SRT. Second, while healthy rabbits were used in this study, an animal model with RPE dysfunction will be needed to investigate the effect of SRT in further studies. RPE restoration after SRT can be affected negatively in diseased RPE cells, because RPE cells obtained from patients with AMD lack growth potential in vitro [39]. Third, the regeneration potential of RPE in animals is thought to be greater than that in humans [23, 40]. Although a small RPE defect could be repaired by RPE proliferation in patients with an RPE tear, a large defect was not covered by RPE proliferation [41]. As SRT was not effective against geographic atrophy, RPE restoration after SRT could be limited by the size of the RPE defect in humans.

In this study, a fixed pulse energy (25 μJ) was used, because the mean real applied energy of SRT (< 25 μJ) induced adequate RPE damage in a previous rabbit experiment [14]. Although this level of irradiation (25 μJ) produced adequate

SRT spots in all cases in this study, fixed pulse energy may not always induce appropriate SRT lesions, due to interindividual variation of retinal pigmentation. Considering that RFD could not detect weak FFA-positive spots (3.9%) in this study, it may be difficult to detect very small SRT lesions with RFD, as reported in a prior study [14]. Our results indicate that the accuracy of RFD could be affected by undertreatment rather than overtreatment. Nevertheless, RFD could be helpful for titrating pulse energy, because no overtreatment effects, such as burns, were observed in this study.

In conclusion, our findings that HD-SRT lesions were fully covered with RPE with microvilli by 1 month after treatment indicate that HD-SRT can strengthen the effect of SRT by enlarging the area of RPE rejuvenation; however, these lesions may heal slower than those induced by LD-SRT.

Authors' contributions Conceived and designed the experiments: Young-Jung Roh; Performed the treatment: Young-Jung Roh; Analyzed the data: Seung Hee Jeon, Minhee Kim, Young-Jung Roh; Contributed reagents/materials/analysis tools: Seung Hee Jeon, Minhee Kim; Wrote the paper: Seung Hee Jeon, Minhee Kim, Young-Jung Roh; Approved final version of the manuscript: Seung Hee Jeon, Minhee Kim, Young-Jung Roh.

Funding information This study was supported by the grant from South Korean Government's Ministry of Trade, Industry and Energy (M000004912–00192937). This animal study was supported by Research Institute of Medical Science of Yeouido St. Mary's hospital.

Data availability Not applicable.

Compliance with ethical standards

Conflict of interest YJ Roh has a patent related to real-time feedback dosimetry in South Korea, which is under the PCT application process. Lutronic and our research team jointly received funds from an international research and development project from the South Korean Government's Ministry of Trade, Industry, and Energy (M000004912-00192937). Lutronic had a role in technical support.

Ethical approval This study followed the ARVO Statement for the Use of Animals in Ophthalmic and Vision Research and was approved by the Institutional Animal Care and Use Committee of the Catholic University of Korea.

Consent to participate Not applicable.

Consent for publication Not applicable.

Code availability Not applicable.

References

1. The Diabetic Retinopathy Study Research Group (1981) Photocoagulation treatment of proliferative diabetic retinopathy. Clinical application of diabetic retinopathy study (DRS) findings, diabetic retinopathy study report number 8. Ophthalmology 88: 583–600
2. Early Treatment Diabetic Retinopathy Study Research Group (1985) Photocoagulation for diabetic macular edema. Early treatment diabetic retinopathy study report number 1. Arch Ophthalmol 103:1796–1806
3. Lim JI (1999) Iatrogenic choroidal neovascularization. Surv Ophthalmol 44:95–111. https://doi.org/10.1016/s0039-6257(99)00077-6
4. Lewis H, Schachat AP, Haimann MH, Haller JA, Quinlan P, von Fricken MA, Fine SL, Murphy RP (1990) Choroidal neovascularization after laser photocoagulation for diabetic macular edema. Ophthalmology 97:503–510; discussion 510-501. https://doi.org/10.1016/s0161-6420(90)32574-5
5. Brinkmann R, Roider J, Birngruber R (2006) Selective retina therapy (SRT): a review on methods, techniques, preclinical and first clinical results. Bull Soc Belge Ophtalmol 302:51–69
6. Park YG, Seifert E, Roh YJ, Theisen-Kunde D, Kang S, Brinkmann R (2014) Tissue response of selective retina therapy by means of a feedback-controlled energy ramping mode. Clin Exp Ophthalmol 42:846–855. https://doi.org/10.1111/ceo.12342
7. Treumer F, Klettner A, Baltz J, Hussain AA, Miura Y, Brinkmann R, Roider J, Hillenkamp J (2012) Vectorial release of matrix metalloproteinases (MMPs) from porcine RPE-choroid explants following selective retina therapy (SRT): towards slowing the macular ageing process. Exp Eye Res 97:63–72. https://doi.org/10.1016/j.exer.2012.02.011
8. Richert E, Koinzer S, Tode J, Schlott K, Brinkmann R, Hillenkamp J, Klettner A, Roider J (2018) Release of different cell mediators during retinal pigment epithelium regeneration following selective retina therapy. Invest Ophthalmol Vis Sci 59:1323–1331. https://doi.org/10.1167/iovs.17-23163
9. Roider J, Brinkmann R, Wirbelauer C, Laqua H, Birngruber R (1999) Retinal sparing by selective retinal pigment epithelial photocoagulation. Arch Ophthalmol 117:1028–1034. https://doi.org/10.1001/archopht.117.8.1028
10. Roider J, Liew SH, Klatt C, Elsner H, Poerksen E, Hillenkamp J, Brinkmann R, Birngruber R (2010) Selective retina therapy (SRT) for clinically significant diabetic macular edema. Graefes Arch Clin Exp Ophthalmol 248:1263–1272. https://doi.org/10.1007/s00417-010-1356-3
11. Park YG, Kim JR, Kang S, Seifert E, Theisen-Kunde D, Brinkmann R, Roh YJ (2016) Safety and efficacy of selective retina therapy (SRT) for the treatment of diabetic macular edema in Korean patients. Graefes Arch Clin Exp Ophthalmol 254:1703–1713. https://doi.org/10.1007/s00417-015-3262-1
12. Park YG, Kang S, Kim M, Yoo N, Roh YJ (2017) Selective retina therapy with automatic real-time feedback-controlled dosimetry for chronic central serous chorioretinopathy in Korean patients. Graefes Arch Clin Exp Ophthalmol 255:1375–1383. https://doi.org/10.1007/s00417-017-3672-3
13. Schuele G, Elsner H, Framme C, Roider J, Birngruber R, Brinkmann R (2005) Optoacoustic real-time dosimetry for selective retina treatment. J Biomed Opt 10:064022. https://doi.org/10.1117/1.2136327
14. Minhee K, Park YG, Kang S, Roh YJ (2018) Comparison of the tissue response of selective retina therapy with or without real-time feedback-controlled dosimetry. Graefes Arch Clin Exp Ophthalmol 256:1639–1651. https://doi.org/10.1007/s00417-018-4067-9
15. Seifert E, Tode J, Pielen A, Theisen-Kunde D, Framme C, Roider J, Miura Y, Birngruber R, Brinkmann R (2018) Selective retina therapy: toward an optically controlled automatic dosing. J Biomed Opt 23:1–12. https://doi.org/10.1117/1.Jbo.23.11.115002
16. Valentino TL, Kaplan HJ, Del Priore LV, Fang SR, Berger A, Silverman MS (1995) Retinal pigment epithelial repopulation in

monkeys after submacular surgery. Arch Ophthalmol 113:932–938. https://doi.org/10.1001/archopht.1995.01100070106033
17. Del Priore LV, Hornbeck R, Kaplan HJ, Jones Z, Valentino TL, Mosinger-Ogilvie J, Swinn M (1995) Debridement of the pig retinal pigment epithelium in vivo. Arch Ophthalmol 113:939–944. https://doi.org/10.1001/archopht.1995.01100070113034
18. Del Priore LV, Kaplan HJ, Hornbeck R, Jones Z, Swinn M (1996) Retinal pigment epithelial debridement as a model for the pathogenesis and treatment of macular degeneration. Am J Ophthalmol 122:629–643. https://doi.org/10.1016/s0002-9394(14)70481-7
19. Oganesian A, Bueno E, Yan Q, Spee C, Black J, Rao NA, Lopez PF (1997) Scanning and transmission electron microscopic findings during RPE wound healing in vivo. Int Ophthalmol 21:165–175. https://doi.org/10.1023/a:1026402031902
20. Sorensen NB, Lassota N, Kyhn MV, Prause JU, Qvortrup K, la Cour M, Kiilgaard J (2013) Functional recovery after experimental RPE debridement, mfERG studies in a porcine model. Graefes Arch Clin Exp Ophthalmol 251:2319–2325. https://doi.org/10.1007/s00417-013-2331-6
21. Kriechbaum K, Bolz M, Deak GG, Prager S, Scholda C, Schmidt-Erfurth U (2010) High-resolution imaging of the human retina in vivo after scatter photocoagulation treatment using a semiautomated laser system. Ophthalmology 117:545–551. https://doi.org/10.1016/j.ophtha.2009.07.031
22. Kiilgaard JF, Prause JU, Prause M, Scherfig E, Nissen MH, la Cour M (2007) Subretinal posterior pole injury induces selective proliferation of RPE cells in the periphery in in vivo studies in pigs. Invest Ophthalmol Vis Sci 48:355–360. https://doi.org/10.1167/iovs.05-1565
23. Framme C, Brinkmann R, Birngruber R, Roider J (2002) Autofluorescence imaging after selective RPE laser treatment in macular diseases and clinical outcome: a pilot study. Br J Ophthalmol 86:1099–1106. https://doi.org/10.1136/bjo.86.10.1099
24. Kang S, Park YG, Kim JR, Seifert E, Theisen-Kunde D, Brinkmann R, Roh YJ (2016) Selective retina therapy in patients with chronic central serous chorioretinopathy: a pilot study. Medicine 95:e2524. https://doi.org/10.1097/md.0000000000002524
25. Yasui A, Yamamoto M, Hirayama K, Shiraki K, Theisen-Kunde D, Brinkmann R, Miura Y, Kohno T (2017) Retinal sensitivity after selective retina therapy (SRT) on patients with central serous chorioretinopathy. Graefes Arch Clin Exp Ophthalmol 255:243–254. https://doi.org/10.1007/s00417-016-3441-8
26. Bonilha VL, Bhattacharya SK, West KA, Crabb JS, Sun J, Rayborn ME, Nawrot M, Saari JC, Crabb JW (2004) Support for a proposed retinoid-processing protein complex in apical retinal pigment epithelium. Exp Eye Res 79:419–422. https://doi.org/10.1016/j.exer.2004.04.001
27. Lamb TD, Pugh EN Jr (2004) Dark adaptation and the retinoid cycle of vision. Prog Retin Eye Res 23:307–380. https://doi.org/10.1016/j.preteyeres.2004.03.001
28. Roider J, Brinkmann R, Wirbelauer C, Laqua H, Birngruber R (2000) Subthreshold (retinal pigment epithelium) photocoagulation in macular diseases: a pilot study. Br J Ophthalmol 84:40–47. https://doi.org/10.1136/bjo.84.1.40
29. Guymer RH, Wu Z, Hodgson LAB, Caruso E, Brassington KH, Tindill N, Aung KZ, McGuinness MB, Fletcher EL, Chen FK, Chakravarthy U, Arnold JJ, Heriot WJ, Durkin SR, Lek JJ, Harper CA, Wickremasinghe SS, Sandhu SS, Baglin EK, Sharangan P, Braat S, Luu CD (2019) Subthreshold nanosecond laser intervention in age-related macular degeneration: the LEAD randomized controlled clinical trial. Ophthalmology 126:829–838. https://doi.org/10.1016/j.ophtha.2018.09.015
30. Chhablani J, Roh YJ, Jobling AI, Fletcher EL, Lek JJ, Bansal P, Guymer R, Luttrull JK (2018) Restorative retinal laser therapy: present state and future directions. Surv Ophthalmol 63:307–328. https://doi.org/10.1016/j.survophthal.2017.09.008
31. Tode J, Richert E, Koinzer S, Klettner A, von der Burchard C, Brinkmann R, Lucius R, Roider J (2019) Selective retina therapy reduces Bruch's membrane thickness and retinal pigment epithelium pathology in age-related macular degeneration mouse models. Transl Vis Sci Technol 8:11. https://doi.org/10.1167/tvst.8.6.11
32. Binder S, Krebs I, Hilgers RD, Abri A, Stolba U, Assadoulina A, Kellner L, Stanzel BV, Jahn C, Feichtinger H (2004) Outcome of transplantation of autologous retinal pigment epithelium in age-related macular degeneration: a prospective trial. Invest Ophthalmol Vis Sci 45:4151–4160. https://doi.org/10.1167/iovs.04-0118
33. Falkner-Radler CI, Krebs I, Glittenberg C, Povazay B, Drexler W, Graf A, Binder S (2011) Human retinal pigment epithelium (RPE) transplantation: outcome after autologous RPE-choroid sheet and RPE cell-suspension in a randomised clinical study. Br J Ophthalmol 95:370–375. https://doi.org/10.1136/bjo.2009.176305
34. Park YG, Kang S, Brinkmann R, Roh YJ (2015) A comparative study of retinal function in rabbits after panretinal selective retina therapy versus conventional panretinal photocoagulation. J Ophthalmol 2015:247259. https://doi.org/10.1155/2015/247259
35. Kim M, Park YG, Jeon SH, Choi SY, Roh Y-J (2020) The efficacy of selective retina therapy for diabetic macular edema based on pretreatment central foveal thickness. Lasers Med Sci https://doi.org/10.1007/s10103-020-02984-6
36. Daruich A, Matet A, Moulin A, Kowalczuk L, Nicolas M, Sellam A, Rothschild P-R, Omri S, Gélizé E, Jonet L, Delaunay K, De Kozak Y, Berdugo M, Zhao M, Crisanti P, Behar-Cohen F (2018) Mechanisms of macular edema: beyond the surface. Prog Retin Eye Res 63:20–68. https://doi.org/10.1016/j.preteyeres.2017.10.006
37. Prahs P, Walter A, Regler R, Theisen-Kunde D, Birngruber R, Brinkmann R, Framme C (2010) Selective retina therapy (SRT) in patients with geographic atrophy due to age-related macular degeneration. Graefes Arch Clin Exp Ophthalmol 248:651–658. https://doi.org/10.1007/s00417-009-1208-1
38. Wang H, Van Patten Y, Sugino IK, Zarbin MA (2006) Migration and proliferation of retinal pigment epithelium on extracellular matrix ligands. J Rehabil Res Dev 43:713–722. https://doi.org/10.1682/jrrd.2005.06.0114
39. van Meurs JC, ter Averst E, Croxen R, Hofland L, van Hagen PM (2004) Comparison of the growth potential of retinal pigment epithelial cells obtained during vitrectomy in patients with age-related macular degeneration or complex retinal detachment. Graefes Arch Clin Exp Ophthalmol 242:442–443. https://doi.org/10.1007/s00417-003-0852-0
40. Rabenlehner D, Stanzel BV, Krebs I, Binder S, Goll A (2008) Reduction of iatrogenic RPE lesions in AMD patients: evidence for wound healing? Graefes Arch Clin Exp Ophthalmol 246:345–352. https://doi.org/10.1007/s00417-007-0658-6
41. Caramoy A, Fauser S, Kirchhof B (2012) Fundus autofluorescence and spectral-domain optical coherence tomography findings suggesting tissue remodelling in retinal pigment epithelium tear. Br J Ophthalmol 96:1211–1216. https://doi.org/10.1136/bjophthalmol-2012-301750

Publisher's note Springer Nature remains neutral with regard to jurisdictional claims in published maps and institutional affiliations.